DTC Versus Vector Control Strategies for a grid connected DFIG based wind turbine

Conference Paper · November 2018

CITATIONS
0

READS
128

2 authors, including:

Kouider Khaled
Université Tahri Mohammed Béchar
10 PUBLICATIONS **0** CITATIONS

SEE PROFILE

DTC Versus Vector Control Strategies for a grid connected DFIG based wind turbine

Kouider Khaled [1], Bekri Abdelkader [1]

[1]*Department of Electrical Engineering, University of Tahri Mohammed* BP 417, Bechar (08000), Bechar, Algeria
khouiledkhaled@gmail.com, bekriabdkader@yahoo.fr

Keywords: Direct torque control, hysteresis, lock-up table, vector control, Stator flux orientation.

Abstract: With the high level of wind power penetration, system executives have an increasing interest in investigating the wind power integration influence on power systems. The doubly fed induction generator (DFIG) is commonly employed in wind power generation systems. In this paper, we focus on the direct torque and the classic vector control applied to the rotor side converter (RSC) of a grid-connected doubly fed induction generator (DFIG) using a detailed dynamic model under dq reference frame. The two strategies are compared considering many parameters as the rotor currents, the stator power, electromagnetic torque and rotor flux to ensure the proper operation and to enhance the performance of the DFIG. Both control strategies of our machine are simulated using MATLAB/SIMULINK software package. Finally, the simulations results are displayed and well discussed..

1 INTRODUCTION

Nowadays, the electrical power consumption increases proportionally with the human society. It's reported by (Enerdata, 2018) that the global net electricity consumption has risen from 21.463 TWh in 2016 to 22.015 TWh in 2017 (the Power consumption accelerated again in 2017 (+2.3%)). Since the major part of electricity is generated from fossil fuels, the increase in net electricity consumption will result in significant greenhouse gas emissions, which could lead to global warming (Dehong et al., 2018). For this reason, the renewable energies occupied a crucial position in the last research. The wind power generation is regarded as the most widely used non-hydro renewable energy generation with a renewable and clean high reserve. Besides, it provides almost no greenhouse gas emissions (Dehong et al., 2018). In the same context, and due to many technical and economic factors like the partial scale converting using an economical converter size to handle a fraction (20-30%) of the total power, the doubly fed induction generator (DFIG) based wind turbine is considered one of the most practical solutions for the wind power conversion. A regular arrangement of a DFIG-WT system is illustrated in Figure 1. A wound rotor induction generator with slip

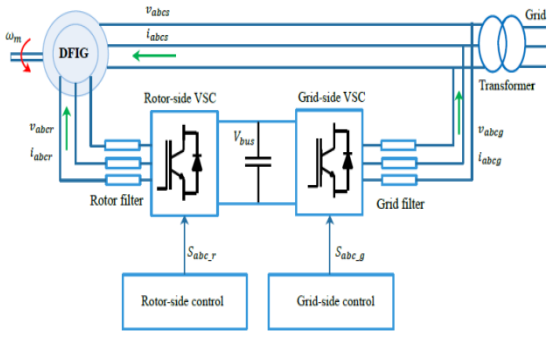

Figure 1: A standard configuration of a doubly fed induction generator (DFIG) wind power system (Haitham et al., 2014).

ring is essential to conduct current toward or out of the rotor winding at slip frequency.

The variable-speed operation is achieved with the help of injecting a controllable rotor voltage (Fox et al., 2014). The DFIG could be operated under 3 modes (Subsynchronous operation when $\boldsymbol{\omega_m < \omega_s}$, Hypersynchronous operation while $\boldsymbol{\omega_m > \omega_s}$, and in Synchronous mode if $\boldsymbol{\omega_m = \omega_s}$,where (ω_s, ω_m are

the synchronous rotor electrical speed) allowing a bidirectional power flow from or into the back-to-back converter. The grid connection of the DFIG-WT receives a big intention in the last decade. Many works are fulfilled such as the classic vector control as in (Dehong et al., 2018), (Fox et al., 2014), (Kerrouche et al., 2013) and (Fei et al., 2012) to enhance the performance of the DFIG wind power systems. In the recent years, the direct control techniques are gained a huge importance as in (Arnalte et al., 2013), and a new improved direct torque control strategy is developed in (Yungui et al., 2016). An ANFIS based DTC for a DFIG is applied in (Kumar et al., 2013). In this paper, we concentrate on the comparison between the direct torque control and the classic vector control methods for a DFIG wind system. For this purpose, this article will be split into three subsections: firstly, the detailed DFIG-WT mathematical model is achieved, then the description of the two control methods laws and equations are established. Finally, the simulation and results are well explained. In this context, this paper reveals that it is possible to compare the performance of both strategies using various parameters.

2 DFIG IN WIND ENERGY CONVERSION SYSTEMS

In this section, the most essential electric and mechanic equations of the DFIG wind system are used to achieve an analytical model proper for the control of the machine. The mathematical modelling of the system is well shown in the two following subsections:

2.1 DFIG mathematical modelling

The dynamic model of the DFIG under dq reference frame can be reached using the stator and rotor windings equations as follows (Gonzalo et al., 2011), (Haitham et al., 2014), and (Zhaoyang et al., 2014), where $\psi_{sd}, \psi_{sq}, \psi_{rd}, \psi_{rq}, i_{sd}, i_{sq}, i_{rd}, i_{rq}$ are the stator and rotor flux and currents under dq components respectively and $R_s, R_r, \omega_s, \omega_r, p$ are the stator and ,rotor resistances and speeds and the number of poles pairs :

$$u_{sd} = R_s i_{sd} + \frac{d\psi_{sd}}{dt} - \omega_s \psi_{sq}$$

$$u_{sq} = R_s i_{sq} + \frac{d\psi_{sq}}{dt} + \omega_s \psi_{sd}$$

$$u_{rd} = R_r i_{rd} + \frac{d\psi_{rd}}{dt} - \omega_r \psi_{rq}$$

$$u_{rd} = R_r i_{rd} + \frac{d\psi_{rd}}{dt} + \omega_r \psi_{rq} \quad (1)$$

After that, the rotor and stator flux are given by eq (2), with L_s, L_r, L_m are the stator, rotor and mutual inductances:

$$\psi_{sd} = L_s i_{sd} + L_m i_{rd}$$

$$\psi_{sq} = L_s i_{sq} + L_m i_{rq}$$

$$\psi_{rd} = L_r i_{rd} + L_m i_{sd}$$

$$\psi_{rq} = L_r i_{rq} + L_m i_{sq} \quad (2)$$

And the electromagnetic torque:

$$T_{em} = \frac{3}{2} p (i_{rd} i_{sq} + i_{rq} i_{sd}) \quad (3)$$

2.2 Aerodynamic turbine modelling

The mechanical power P_m received from the wind can be denoted by the complex algebraic equation in function of blade pitch angle β, the rotor blades diameter and the Air density R, ρ, shaft and wind speed Ω_t, V_w,the tip speed ratio λ and the power coefficient C_p as shown in (4):

$$P_m = \frac{1}{2} \rho \pi R^2 {V_w}^3 C_p(\lambda, \beta) \quad (4)$$

With λ is the tip speed ratio $\lambda = \frac{R\Omega_t}{V_w}$ (5)

In this paper we use C_{pmax} = 0.44 and $\lambda_{opt} = 7.2$.

The gearbox is an essential part of the wind turbine systems. They usually used to adapt the low rotor shaft speed Ω_t to the high speed of the generator Ω_m. The following equations describe it in addition to the mechanical speed evolution:

$$\begin{cases} T_m = \frac{T_{aer}}{G} \\ \Omega_t = \frac{\Omega_m}{G} \end{cases} \quad (6)$$

$$J \frac{d\Omega_m}{dt} = T_m - T_{em} - f\Omega_m \quad (7)$$

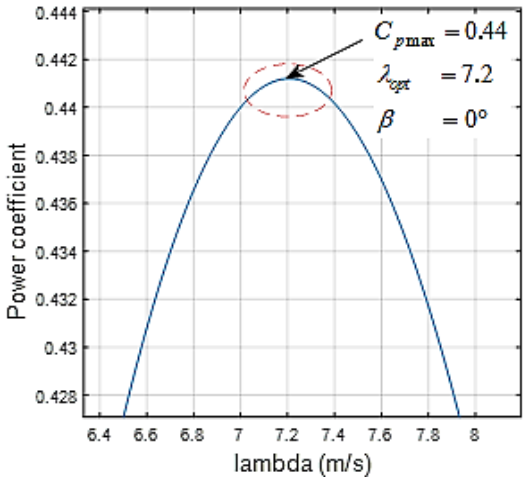

Figure 2: The Power coefficient C_pVersus the Tip Speed Ratio λ.

3 CONTROL TECHNIQUES OF THE DFIG

As mentioned before, the control strategies used in this paper are: the classic vector control and the direct torque control. Both approaches will be well described in the succeeding two subsections.

3.1 Classic vector control

Numerous control approaches are applied for the DFIG control, despite of that, the vector control techniques were the most established ones. The use of the dq synchronous reference frame is ordinarily shared between the DFIG and the other machines (Bin et al., 2011).

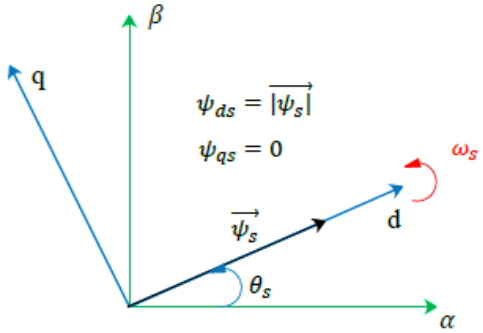

Figure 3: stator flux-oriented in the dq reference frame

From the previous dynamic model of the DFIG, and basing on the d-axis alignment of the stator flux($\psi_{qs} = 0$), we obtain the two rotor voltage equations:

$$u_{rd} = R_r i_{rd} + \sigma L_r \frac{di_{rd}}{dt} - \omega_r L_r i_{rq} + \frac{L_m}{L_s}\frac{d}{dt}\overrightarrow{|\psi_s|} \quad (8)$$

$$u_{rq} = R_r i_{rq} + \sigma L_r \frac{di_{rq}}{dt} - \omega_r L_r i_{rd} + \omega_r \frac{L_m}{L_s}\frac{d}{dt}\overrightarrow{|\psi_s|} \quad (9)$$

Where σ is the Blondel's coefficien $\sigma = 1 - \frac{{L_m}^2}{L_r L_s}$

Basing on the d-axis alignment as shown in the Figure 3, we see that the reactive power $Q_s$is directly affected by the current I_{dr}, while the current I_{qr} modified the torque/active power (Haitham et al., 2014)as shown in equations (10) and (11):

$$T_{em} = \frac{3}{2}p\left(\psi_{qs} i_{dr} - \psi_{ds} i_{qr}\right) \Rightarrow T_{em} = -\frac{3}{2}p\frac{L_m}{L_s}\overrightarrow{|\psi_s|} i_{qr} \quad (10)$$

$$Q_s = -\frac{3}{2}\omega_s \frac{L_m}{L_s}\overrightarrow{|\psi_s|}\left(i_{dr} - \frac{\overrightarrow{|\psi_s|}}{L_m}\right) \quad (11)$$

A detailed explanation of the vector control technique and the current control loops used in this strategy are well established in (Haitham et al., 2014). Furthermore, the complete vector control schema used in this paper is well drawn in Figure 4.

3.2 Direct torque control principles for the DFIG

The direct control strategies are recognized like the modern solutions for the AC drives. Usually, from the side of the performance and global features, and compared to the vector control strategies, there are many differences. Several works have fulfilled in this area in (Gonzalo et al., 2011), (Zhang et al., 2011), (Jihène et al., 2011) and (Xiong et al., 2016), and as a consequence, various contributions to these new techniques are tested for a proper DFIG based wind turbine applications.

Referring to (Haitham et al., 2014), many facts about the DTC Principle can be extracted: first, two variables of the DFIG have immediately commanded: the amplitudes of both rotor flux and the electromagnetic torque. Moreover, the angle δ denotes the distance between both stator and rotor

flux vectors and by adjusting this angle we can control the torque. Furthermore, with the help of the injection of different voltage vectors to the rotor of the DFIG, the rotor flux trajectory and amplitude can be directly modified using a 2-level voltage source converter (VSC). Eventually, The DTC is nearly related to the VSC that is manipulated. Therefore, the pulses are generated directly without any modulation schema.

Two hysteresis comparators are used in the Classic DTC, one for the flux controller and it is based on 2-level hysteresis comparator with the band HF, and the other is based on 3-level hysteresis comparator HT for the electromagnetic torque. Practically, the bands values are usually restricted using the lowest switching sample time of the implementation tools (Adel et al., 2010). The Figure 5. Shows the two hysteresis controller for both flux and torque.

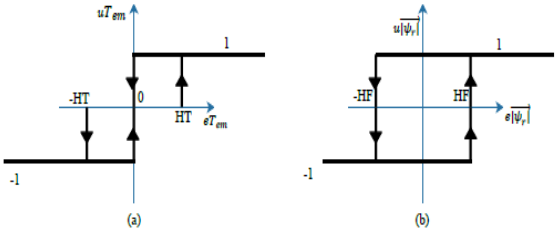

Figure 5: (a) 3 level hysteresis comparator for the torque, (b) 2 level hysteresis comparator for the rotor flux.

After recognizing the fundamental principle of the DTC, the next step is to estimate the main variables of the control technique (Tem, Rotor flux and the rotor flux angle), which can be described directly by the following equations:

$$T_{em} = \frac{3}{2} p \frac{L_m}{\sigma L_r L_s} \overrightarrow{|\psi_r|} \overrightarrow{|\psi_s|} sin\delta \qquad (12)$$

$$\psi_{rd} = \int_0^t (V_{rd} - R_r I_{rd})$$

$$\psi_{rq} = \int_0^t (V_{rq} - R_r I_{rq}) \qquad (13)$$

$$\overrightarrow{|\psi_r|} = \sqrt{{\psi_{rd}}^2 + {\psi_{rq}}^2} \qquad (14)$$

Besides, after the computation of the rotor flux dq components, it is necessary to determine the rotor flux angle $\theta_{\psi r}$, then the sectors can be simply calculated.

$$\theta_{\psi r} = atan\left(\frac{\psi_{rq}}{\psi_{rd}}\right) \qquad (15)$$

The eight space voltage vectors are calculated using:

$$\begin{cases} V_i = \frac{2}{3} V_{dc} e^{-j\frac{\pi}{3}(i-1)} \\ V_0 = V_7 = 0 \end{cases} \qquad (16)$$

With i is the sector number where $i = [1 \dots 6]$.

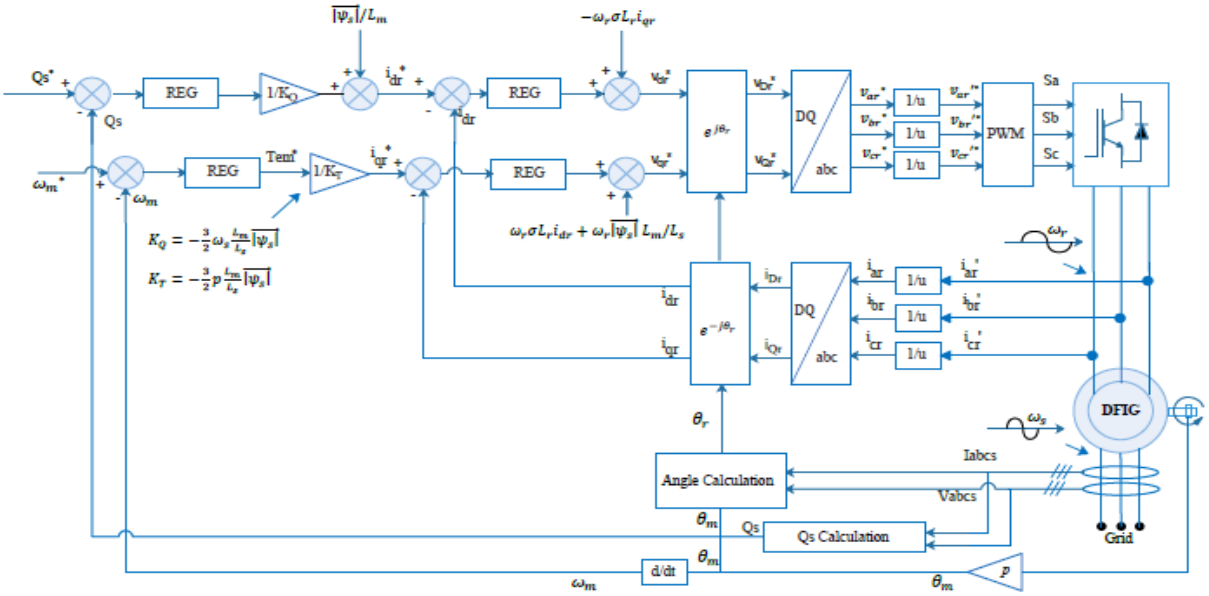

Figure 4. The overall vector control diagram applied to the rotor side converter (RSC) of the DFIG (Haitham et al., 2014).

Then, the selection of the proper rotor space vector is done based on Table 1.

Table 1: Rotor voltage vector selection according to torque and flux errors.

		uTem		
		1	0	-1
$u\overrightarrow{\lvert\psi_r\rvert}$	1	$V_{(i-1)}$	V_0, V_7	$V_{(i+1)}$
	0	$V_{(i-1)}$	V_0, V_7	$V_{(i+1)}$

Finally, the entire diagram of the DTC for DFIG wind system is well depicted in Figure 6.

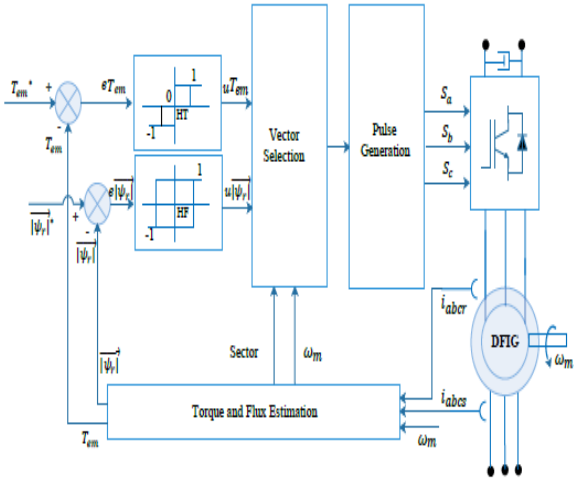

Figure 6. DTC diagram applied to the RSC of the DFIG (Gonzalo et al., 2011).

4 SIMULATION AND RESULTS

The simulation is made using the MATLAB/SIMULINK software package to examine the DTC and vector control strategies performance for a 2MW DFIG-WT described in the appendix.

In this paper , two control strategies(DTC and the classic vector control) will be compared to discuss the performance of a 2MW DFIG-WT. 4 parametres will be investigated (the electromagnetique torque T_{em}, the rotor flux ψ_r, the rotor current I_r,the stator power P_s).

For the simulation of both control strategies,we use the magnetisation through the stator ($I_{dr} = 0$), all the parametres used in this simulation are well cited in the Appendix.

4.1 vector control simulation

The Figures (from 7 to 10) shows the essential rotor side converter (RSC) variables (rotor currents, rotor flux ,the electromagnetic torque and the stator power).From the Figure. 7(a) and Figure. 7(b) we see that the direct and the quadratic components of the rotor currents follow the references after nearly 3 seconds after a transient.

The rotor flux amplitude and the electromagnetic torque are shown by the Figure. 8 and Figure. 9, after the transient state the two variables remain stable state after nearly 5 seconds and the electromagnetic torque coincide with the reference at that time.

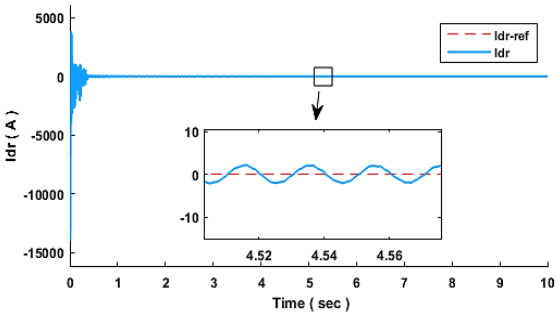

(a)

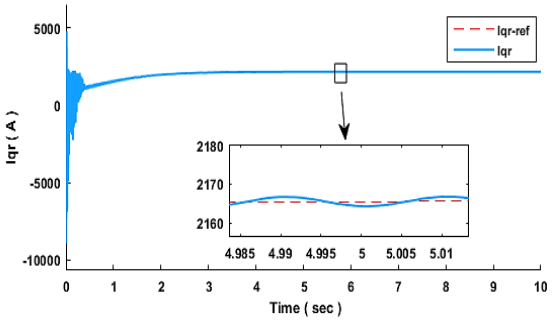

(b)

Figure 7. Dq rotor currents components versus references, (a) direct component,(b) quadratic component.

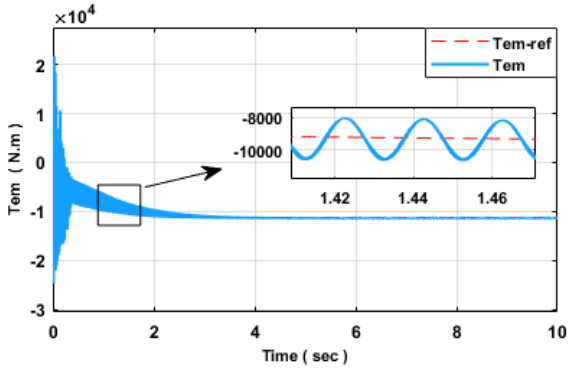

Figure 8: Electromagnetic torque versus the reference.

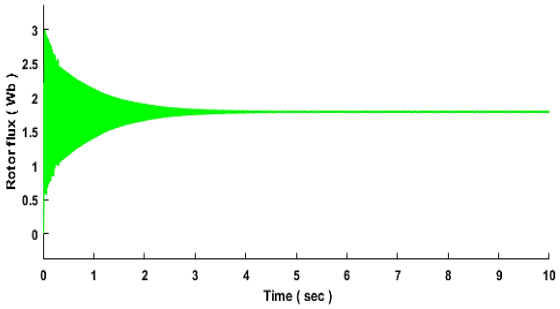

Figure 9: Rotor flux magnitude.

Furthermore, the power delivered by the stator is well illustrated in the Figure. 10, we see that the power after the starting state increased until achieving 1.77 MW at permanent.

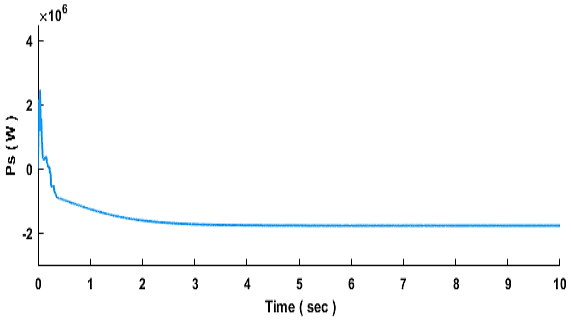

Figure 10: The stator power.

4.2 Direct torque control simulation

In this part, the same parameters of the vector control except the rotor currents will be treated. Besides, the following Figures (11-12) shows the rotor flux amplitude and the electromagnetic torque, starting with rotor flux amplitude which follows the reference ($\psi_{r-ref} = 0.96\, wb$) fastly as shown in Figure .11. Moreover, the Figure .12 demonstrates how the torque matches the reference rapidly with a neglected error, and both zooms confirm that.

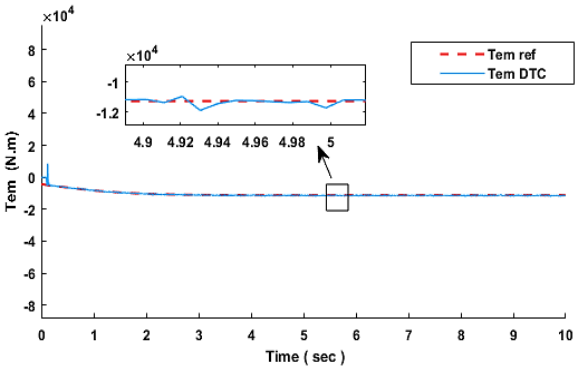

Figure 11: Electromagnetic torque versus the reference.

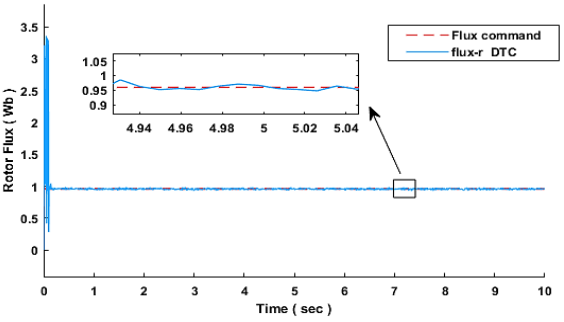

Figure 12. The rotor flux magnitude versus the reference.

The Figure .13 displays the stator power delivered to the grid, and we see that after a transient starting, the stator power achieve 1.65MW at steady state.

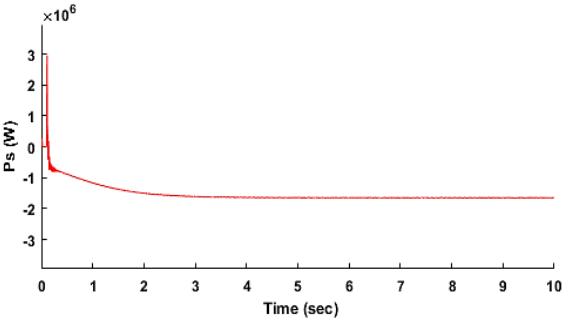

Figure 13. The stator power.

4.3 Comparative Studies

In this section, only the electromagnetic torque and the stator power will be compared between both

control techniques. The Figure .14 illustrates the developed electromagnetic torque for the two strategies, and it is clear that the DTC technique coincides with the reference rapidly than the vector control. Besides, the power delivered from the stator for both strategies is shown by Figure .15.It is well demonstrated that the vector control has more power (1.77MW) than the DTC (1.65 MW), knowing that in this paper we use the generator convention, so the negative sign means generating mode.

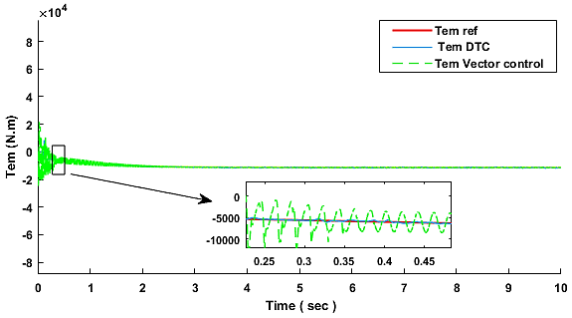

Figure 14: The Electromagnetic torque comparaison.

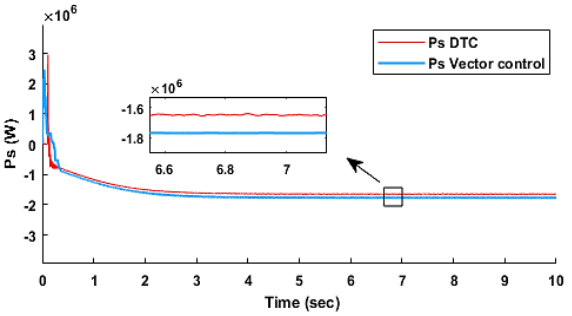

Figure 15: The stator power comparaison.

5 CONCLUSION

In this paper, a comparative study between the vector control and the direct torque control (DTC) strategies applied for the rotor side converter (RSC) has been demonstrated. The classic vector control needs many control loops with PI controllers to generate references, but in contrast, it delivered power more than the DTC control. With regard to the DTC, it has a simple configuration and a fast response for both flux and torque, but producing more power losses due to the variable switching frequency. Finally, this study can afford a good support for proper control and operation of the machine in term of performance and complexity of the chosen control techniques.

REFERENCES

Enerdata (2018). The Global Energy Statistical Yearbook. https://yearbook.enerdata.net . Accessed: 13-Oct-2018.

Dehong, X., Frede, B., Wenjie, C., and Nan, Z. (2018). Advanced Control of Doubly Fed Induction Generator for Wind Power Systems. John Wiley & Sons, New Jersey.

Fox, B., Leslie, B., Damian, F., Nick, J., David, M., Mark, O., Richard, W., and Olimpo, A. (2014). Wind Power Integration: Connection and System Operational Aspects, Institution of Engineering and Technology. 2nd Edition, London.

Kerrouche, K., Mezouar, A., and Belgacem, Kh. (2013). Decoupled Control of Doubly Fed Induction Generator by Vector Control for Wind Energy Conversion System.. In *Energy Procedia*, pages: 239-248.

Fei G., Tao, Z., and Zengping, W. (2012). Comparative study of direct power control with vector control for rotor side converter of DFIG, In *9th IET International Conference on Advances in Power System Control, Operation and Management* ,pages.1-6.

Arnalte, S., Burgos, J. C., and Rodríguez-Amenedo, J. L. (2013). Direct Torque Control of a Doubly-Fed Induction Generator for Variable Speed Wind Turbines." *Electric Power Components and Systems* 30(2), pages.199-216.

Yungui, Li., Lijun, Hang., Guojie, Li., Yajuan, Guo., Yunfeng,, Zou., J. Chen., Jun, Li., Jian, Z,. and S. Li. (2016). An improved DTC controller for DFIG-based wind generation system.. In *IEEE 8th International Power Electronics and Motion Control Conference (IPEMC-ECCE Asia)*, pages. 1423-1426.

Kumar, A., and GiriBabu , D. (2016) . Performance improvement of DFIG fed Wind Energy Conversion system using ANFIS controller. In *2nd International Conference on Advances in Electrical, Electronics, Information, Communication and Bio-Informatics (AEEICB)*, pages. 202-206.

Gonzalo A., Jesus. L., Miguel, A,R., Luis, and M., Grzegorz, I. (2011). Doubly fed induction machine

modeling and control for wind energy generation .John Wiley & Sons, New Jersey.

Haitham, A., Mariusz., and M., Kamal , A. (2014). Power Electronics for Renewable Energy Systems, Transportation and Industrial Applications. John Wiley & Sons, Inc. 1st Edition, United Kingdom.

Zhaoyang, S., Ping, W., and Pengxian, S. (2014). Research on control strategy of DFIG rotor side converter. In *IEEE Conference and Expo Transportation Electrification Asia-Pacific (ITEC Asia-Pacific)* ,pages.1-5.

Bin, W, Yongqiang, L., Navid, Z., and Samir, K. (2011). Power Conversion and Control of Wind Energy Systems. John Wiley & Sons, New Jersey.

Zhang , Y., Li, Z., Wang , T., Xu, W., and Zhu , J. (2011). Evaluation of a class of improved DTC method applied in DFIG for wind energy applications. In *International Conference on Electrical Machines and Systems*, pages. 1-6.

Jihène B., Adel, K., and Mohamed, F,M. (2011). DTC, DPC and Nonlinear Vector Control Strategies Applied to the DFIG Operated at Variable Speed. *Journal of Electrical Engineering*, 11(3), pages: 1-13.

Xiong, P. and Sun, D. (2016). Backstepping-Based DPC Strategy of a Wind Turbine Driven DFIG Under Normal and Harmonic Grid Voltage. IEEE Transactions on power Electronics, 31(6), pages: 4216-4225.

Adel, K., and Mohamed, F,M. (2010) "Sensorless-adaptive DTC of double star induction motor." Energy Conversion and Management, 51(12), pages: 2878-2892.

APPENDIX

DFIG-WT parametres:

Vs(line-line) =690V, f=50 hz, P_{nom}= 2MW, Vr(line-line) = 2070 V, P =2, u = 1/3, Is =1070A , (max slip) smax =1/3, (Rated) T_{em}=12732 N.m , Fs =1.9733 Wb , Rs = 0.0026Ω, Rr = 0.0029 Ω , Ls=Lr=0.0026 H , L_m=0.0025 H , β=0, J= 127 kg.m^2 ,f = 0.001, σ = 0.0661, V_{dc}= 1150 V ,R=42, ρ=1.1225 , G=100 . K_{opt}= 270000, ns=synchronous speed =1500 rev/min, s=0.000002 s, V_w=12m/s, (initial slip)=0.2.

Parametres of the DTC:

Ts_DTC=0.00002 s HT=HF=1%.

Parametres of the PI controllers:

Kp_id = Kp_iq = 0.5771, Ki_id = Ki_iq = 491.6

Kp_n =10160 , Ki_n = 406400.